Investigation of Dissociative Electron Transfer Mechanisms and Reactivity Patterns through Kinetic Amplification by a Chain Process

Cyrille Costentin, Philippe Hapiot, Maurice Médebielle, and Jean-Michel Savéant*

Contribution from the Laboratoire d'Electrochimie Moléculaire, Unité Mixte de Recherche Université - CNRS No 7591, Université de Paris 7 - Denis Diderot, Case Courrier 7107, 2 place Jussieu, 75251 Paris Cedex 05, France

Received February 28, 2000

Abstract: The kinetic amplification offered by the $S_{RN}1$ chain process allows the investigation of initiation electron-transfer/bond-breaking steps under very unfavorable thermodynamic conditions, which escape standard kinetic methods. Combining these observations with those derived under conventional thermodynamic conditions allows a considerable extension of the driving force window and thus opens the possibility of uncovering new mechanistic and reactivity patterns. The "thermal" $S_{RN}1$ reaction of 4-nitrobenzyl chloride with 2-nitropropanate ions is an illustrating example where two problems of current interest could be investigated. One of these concerns the actively investigated and debated question of the dichotomy and connections between S_N2 reactions and single electron transfer, particularly the question of catalysis of dissociative electron transfer that may result from mechanism bifurcation along an S_N2 pathway. The other deals with the existence and magnitude of attractive interactions between fragments within the solvent and the influence of these interactions on the dynamics of dissociative electron transfer. Testing systematically the various mechanistic possibilities through simulation of product distribution and half-reaction time led to the conclusion that a small but sizable interaction between fragments within the solvent cage does exist and influences the dynamics of the dissociative electron-transfer reaction quite significantly. While similar effects have been uncovered or suspected in the electrochemical reductions of CCl_4, of other benzyl halides and of phenacyl halides, the reduction of 4-nitrobenzyl chloride by the 2-nitropropanate ion provides a first example of the influence of an interaction between caged fragments on the dynamics of an homogeneous dissociative electron-transfer reaction. The simulations required a precise determination of the various rate constants involved in the chain process. Most of them were derived from cyclic voltammetry and redox catalysis. Particular care was exerted to estimate the ranges of uncertainty on these determinations and hence evaluate the reliability of the mechanistic conclusions.

The reactivity amplification resulting from the chain character of $S_{RN}1$ processes (Scheme 1)[1,2] may be exploited as a tool for investigating mechanisms and reactivity patterns of electron-transfer reactions associated with the breaking of a bond, possibly uncovering new aspects that escaped characterization by other means. A first successful illustration of this strategy has been recently reported.[3] It dealt with the reaction of

Scheme 1

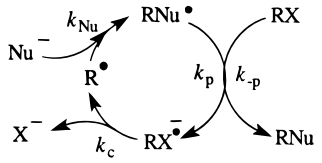

The $S_{RN}1$ Propagation Chain

4-nitrocumyl chloride with 2-nitropropanate ion and as an example illustrating the passage from a concerted to a stepwise mechanism upon increasing the driving force for a homogeneous electron-transfer reaction accompanied by the breaking of a bond. While most of $S_{RN}1$ substitutions require an external stimulation in which a catalytic amount of electrons is injected into the system,[4] in such "thermal" $S_{RN}1$ reactions, the electron donor is the nucleophile that thus serves both as electron-donor initiator of the chain process and as nucleophile in the attack of the radical in the chain process (Schemes 1 and 2). In this example, the amplification offered by the chain process allowed the determination of electron-transfer rate constants as low as

(1) (a) Kerber, C. R.; Urry, G. W.; Kornblum, N. *J. Am. Chem. Soc.* **1965**, *87*, 4520. (b) Kornblum, N.; Michel, R. E.; Kerber, C. R. *J. Am. Chem. Soc.* **1966**, *88*, 5662. (c) Russell, G. A.; Danen, W. C. *J. Am. Chem. Soc.* **1966**, *88*, 5663. (d) Kornblum, N. *Angew. Chem., Int. Ed. Engl.* **1975**, *14*, 734.

(2) (a) Bunnett, J. F. *Acc. Chem. Res.* **1978**, *11*, 413. (b) Savéant, J.-M. *Acc. Chem. Res.* **1980**, *13*, 323. (c) Rossi, R. A.; Rossi, R. H. Aromatic Substitution by the $S_{RN}1$ Mechanism. In *ACS Monograph 1978*; The American Chemical Society: Washington, DC, 1983. (d) Russel, G. A. *Adv. Phys. Org. Chem.* **1987**, *24*, 271. (e) Bowman, W. R. *Chem. Soc. Rev.* **1988**, *17*, 283. (f) Savéant, J.-M. Single Electron Transfer and Nucleophilic Substitution. In *Advances in Physical Organic Chemistry*; Bethel, D., Ed.; Academic Press: New York, 1990; Vol. 26, pp 1−130. (g) Rossi, R. A.; Pierini, A. B.; Palacios, S. M. Nucleophilic Substitution by the $S_{RN}1$ Mechanism on Alkyl Halides. In *Advances in Free Radical Chemistry*; JAI Press: New York, 1990; Vol. 1, pp 193−252. (h) Savéant, J.-M. *Acc. Chem. Res.* **1993**, *26*, 455. (i) Austin, E.; Ferrayoli, C. G.; Alonso, R. A.; Rossi, R. A. *Tetrahedron* **1993**, *49*, 4495. (j) Savéant, J.-M. *J. Phys. Chem.* **1994**, *98*, 3716. (k) Savéant, J.-M. *Tetrahedron* **1994**, *50*, 10117. (l) Rossi, R. A.; Pierini, A. B.; Peñéñory, A. B. Recent Advances in the $S_{RN}1$ Reaction of Organic Halides. In *The Chemistry of Halides, Pseudo-Halides and Azides*; Patai, S., Rappoport, Z., Eds.; Wiley: New York, 1995; Vol. 24, pp 1395−1485. (m) Galli, C.; Gentili. *J. Chem. Soc., Perkin Trans. 2* **1993**, 1135.

(3) Costentin, C.; Hapiot, P.; Médebielle, M.; Savéant, J.-M. *J. Am. Chem. Soc.* **1999**, *121*, 4451.

(4) Solvated electrons in liquid ammonia,[2a] sodium amalgam in the same solvent,[2i] light,[2a,c] electrodes,[2b] electrogenerated electron donors,[2f,g] ferrous salts.[2m]

10.1021/ja000708d CCC: $19.00
Published on Web 05/26/2000

Scheme 2

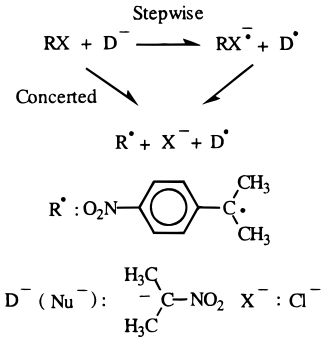

10^{-6} M^{-1} s^{-1}, corresponding to very unfavorable thermodynamics (standard free energy of reaction of the order of +0.4 eV). Electron transfer to the same cleaving substrate could thus be investigated over a very extended domain of driving forces, ranging from this very uphill situation to the conditions that can be reached in electrochemistry and in redox catalysis[5] (the variation of the standard free energy of reaction may reach −1.2 eV), thus allowing the discovery of the first unambiguous transition from a concerted to a stepwise mechanism upon increasing the driving force in an homogeneous electron transfer/bond breaking reaction.[6] As a contribution to the theory of chemical reactivity, this finding together with similar observations concerning electrochemical reactions[6] showed that a mechanism is concerted not necessarily because the intermediate "does not exist" but possibly because the concerted pathway is energetically more advantageous than the stepwise pathway even though the intermediate does exist and can be detected under different driving force conditions. Another outcome of this study was the resolution of the riddle of why this "thermal" $S_{RN}1$ reaction works with such a poor electron donor as initiator.

In the present report, we address two other problems of general interest, taking again advantage of the kinetic amplification offered by the $S_{RN}1$ process.

One of these is the actively investigated and debated question of the dichotomy and connections between S_N2 reactions and single electron transfer. More precisely, is it possible to detect, thanks to the $S_{RN}1$ amplification, the small amount of catalysis[7a] of the electron-transfer process by the S_N2 pathway that may result from mechanism bifurcation?[7b,c]

The other deals with the existence and magnitude of attractive interactions between fragments within the product cluster and

Scheme 3

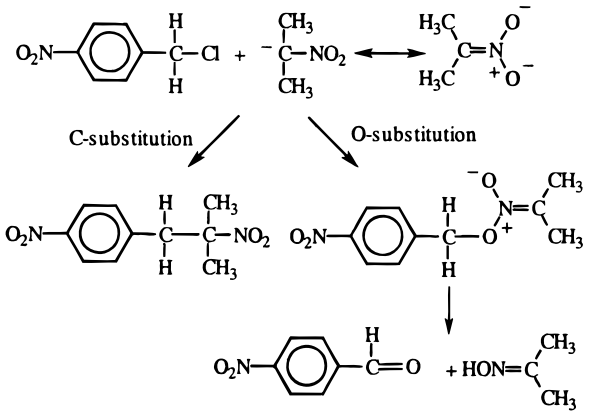

with the influence of these interactions on the dynamics of dissociative electron transfer. There is indeed indirect experimental evidence that such attractive interactions, of the charge/dipole type, may exist in the gas phase after injection of an electron in alkyl halides.[8,9] Ab initio calculations give contrasting results depending on the method used and approximations made.[10−12] It is usually assumed that these interactions vanish in polar solvents. One such case is the anionic state of CF_3Cl,[11] where the shallow minimum calculated in the gas-phase disappears upon solvation, at least when a simple continuum solvation model is used. The attractive interaction existing in the gas phase may persist, even weakened, in the caged product system in a polar solvent and thus influence the dynamics of the concerted and stepwise pathways. Theory[13] indicates that large kinetic effects are expected with relatively weak interactions, and experimental evidence of such effects has recently been gathered in the reduction of carbon tetrachloride.[13a]

The investigation of the reaction of 2-nitropropanate ions with 4-nitrobenzyl chloride (Scheme 3) and comparison of the results with those obtained earlier with 4-nitrocumyl chloride offer a good opportunity to address the two above problems using the $S_{RN}1$ kinetic amplification. The main product is the C-substituted product resulting from the chain reaction depicted in Scheme 1 while the O-substitution product is formed according to a conventional S_N2 reaction. The $S_{RN}1$ character of this Kornblum−Russell reaction[1a−c] is attested by the depressing effect of electron traps such as dinitrobenzene.[1] It may be envisaged that the S_N2 O-substitution reaction could bifurcate toward the dissociative electron transfer, thus producing a small amount of 4-nitrobenzyl radicals that would fuel the propagation loop possibly more efficiently than the very uphill outersphere electron-transfer/bond-breaking reaction. Concerning the second problem, interactions between the caged fragments resulting from dissociative electron transfer are favored by the presence of NO_2 as electron-withdrawing group in the para position. Its effect is not thwarted in the present case, as it is in the 4-nitrocumyl case, by the steric and electronic effect of two methyl groups. As another outcome of this analysis, should be, in this case too, an answer to the question of why this "thermal"

(5) (a) Nadjo, L.; Savéant, J.-M. *J. Electroanal. Chem.* **1973**, *48*, 113. (b) Andrieux, C. P.; Savéant, J.-M. In *Electrochemical Reactions in Investigation of Rates and Mechanism of Reactions, Techniques of Chemistry*; Bernasconi, C. F., Ed.; Wiley: New York, 1986; Vol. VI/4E, Part 2, pp 305−3910. (c) Andrieux, C. P.; Hapiot, P.; Savéant, J.-M. *Chem. Rev.* **1990**, *90*, 723.

(6) (a) As predicted on theoretical grounds[6b] and illustrated by several electrochemical examples.[6c−g] The occurrence of the same phenomenon in homogeneous reaction has given rise to contradictory reports.[6h,i] (b) Andrieux, C. P.; Savéant, J.-M. *J. Electroanal. Chem.* **1986**, *205*, 43. (c) Andrieux, C. P.; Robert, M.; Saeva, F. D.; Savéant, J.-M. *J. Am. Chem. Soc.* **1994**, *116*, 7864. (d) Andrieux, C. P.; Le Gorande, A.; Savéant, J.-M. *J. Electroanal. Chem.* **1994**, *377*, 191. (e) Antonello, S.; Maran, F. *J. Am. Chem. Soc.* **1997**, *119*, 12595. (f) Pause, L.; Robert, M.; Savéant, J.-M. *J. Am. Chem. Soc.* **1999**, *121*, 7158. (g) Antonello, S.; Maran, F. *J. Am. Chem. Soc.* **1999**, *121*, 9668. (h) Severin, M. G.; Farnia, E.; Vianello, E.; Arévalo, M. C. *J. Electroanal. Chem.* **1988**, *251*, 369. (i) Jakobsen, S.; Jensen, H., Pedersen, S.; Daasbjerg, K. *J. Phys. Chem. A* **1999**, *103*, 4141.

(7) (a) Marcus, R. A. *J. Phys. Chem. A* **1997**, *101*, 4072. (b) Shaik, S.; Danovich, D.; Sastry, G. N.; Ayala, P. Y.; Schlegel, H. B. *J. Am. Chem. Soc.* **1997**, *119*, 9237. (c) Costentin, C.; Savéant, J.-M. *J. Am. Chem. Soc.* **2000**, *122*, 2379. (d) It as been shown[7b,c] that the S_N2 reaction with its possible bifurcation is satisfactorily described by means of only the two coordinates shown in Figure 3.

(8) Wentworth, W. E.; George, R.; Keith, H. *J. Chem. Phys.* **1969**, *51*, 1791.

(9) Marcus, R. A. *Acta Chem. Scand.* **1998**, *52*, 858.

(10) Benassi, R.; Bernardi, F.: Bottoni, A.; Robb, M. A.; Taddei, F. *Chem. Phys. Lett.* **1989**, *161*, 79.

(11) Tada, T.; Yoshimura, R. *J. Am. Chem. Soc.* **1992**, *114*, 1593.

(12) Bertran, J.; Gallardo, I.; Moreno, M.; Savéant, J.-M. *J. Am. Chem. Soc.* **1992**, *114*, 9576.

(13) (a) Pause, L.; Robert, M.; Savéant, J.-M., submitted. (b) Costentin, C.; Robert, M.; Savéant, J.-M. *J. Phys. Chem.*, in press.

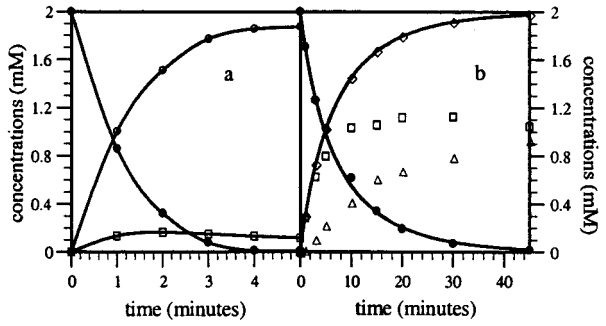

Figure 1. Reaction of 4-nitrobenzyl chloride (2 mM) with tetramethylammonium 2-nitropropanate (4 mM) in the absence (a) and presence (b) of di-*tert*-butyl nitroxide (1.62 mM). Variation of the concentrations with time: ●, 4-nitrobenzyl chloride; ○, C-substitution product; □, 4-nitrobenzaldehyde; △, 4-nitrobenzaldehyde pinacol (concentration multiplied by 2); ◇, sum of □ and △. The reaction is carried out under argon, in the dark at 20 °C.

$S_{RN}1$ reaction (actually the first reported example of a $S_{RN}1$ reaction) works with such a poor electron donor as initiator.

Scheme 4

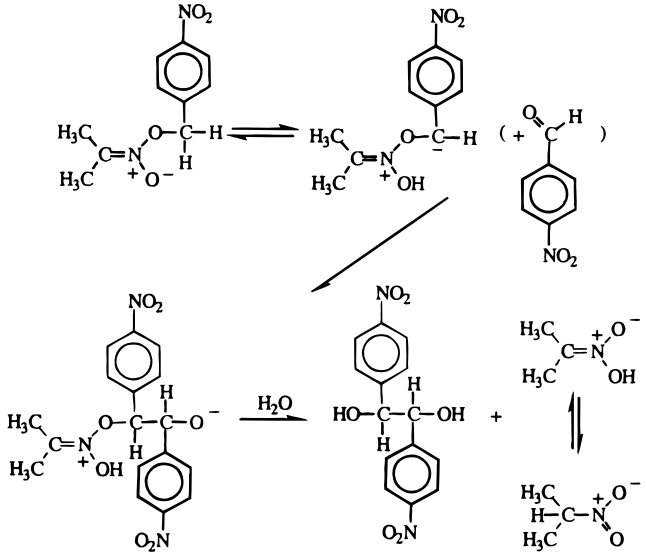

Results and Discussion

Our line of argument involves the following steps. (1) Determination of the reaction kinetics and distribution of products in the absence and presence of a radical trap. These are the data that will serve as reference for testing successively the various possible initiation mechanisms. (2) Derivation of the kinetics of each steps of the propagation loop from direct and indirect electrochemical experiments. The rate constants of the termination steps are estimated from literature sources. These rate constants are essential for testing the initiation mechanisms by means of kinetic simulations. The incidence of uncertainties affecting these rate constants on the accuracy of the simulations and therefore on the reliability of conclusions will be established. On these bases, the following possible initiation mechanisms will be successively evaluated. (3) Outersphere electron transfer followed by bond cleavage. (4) Dissociative electron transfer with negligible interactions between caged fragments. (5) Initiation by the oximate ion produced in the S_N2 O-substitution reaction. (6) Initiation through mechanism bifurcation in the S_N2 O-substitution reaction. (7) Attractive interaction between caged fragments in the dissociative electron-transfer initiation.

1. Reaction Kinetics and Product Distribution. The reaction of 4-nitrobenzyl chloride (2 mM) with tetramethylammonium 2-nitropropanate (4 mM) yields the C-substitution product, (93 ± 1)%, and a small amount of 4-nitrobenzaldehyde, (7 ± 1)%, following the kinetics shown in Figure 1a. We note that the kinetics (half-reaction time ≤ 1 min[14a]) are faster than with 4-nitrocumyl chloride (by at least a factor of 40). As checked in a blank experiment, 4-nitrobenzaldehyde reacts slowly with the 2-nitropropanate ions. It is thus easy to correct the 4-nitrobenzaldehyde points for this small decay as done in Figure 1a. In these experiments, the 2-nitropropanate ions are generated from 2-nitropropane by slightly incomplete irreversible[14b] neutralization with tetramethylammonium hydroxide in order to avoid the deleterious presence of the hydroxide during the course of the $S_{RN}1$ reaction. In the experiment shown in Figure 1a, the concentration of 2-nitropropane was 2.66 mM. We carried out additional experiments with 2-nitropropane concentrations of 4 and 275 mM and observed that the increase of the 2-nitropropane concentration had no noticeable influence on the reaction. We will use this observation in step 5 of the discussion below.

If the reaction is run in the presence of di-*tert*-butyl nitroxide used as a radical trap (Figure 1b), the decay of 4-nitrobenzyl chloride is significantly slower (half-reaction time: 4.8 min) and the formation of the C-substitution product is completely quenched at the benefit of two products deriving from the O-substitution product, namely, 4-nitrobenzaldehyde and its pinacol, according to the mechanism depicted in Schemes 3 and 4. For the following reasons, the mechanism for the formation of the pinacol depicted in Scheme 4 is much more likely than a mechanism that would involve dimerization of two anion radicals of 4-nitrobenzaldehyde produced by electron transfer from the 2-nitropropanate ion to 4-nitrobenzaldehyde. The later reaction is largely endergonic leading to an estimated rate constant smaller than 3×10^{-6} M^{-1} s^{-1} for the formation of the pinacol and thus to half-reaction time larger than 5×10^6 min.[15] The formation of the pinacol along this pathway is thus negligible as confirmed by the fact that no pinacol is detected in the reaction 4-nitrobenzaldehyde with 2-nitropropanate ions which exclusively yields the coupling product. The fact that no pinacol is detected when the reaction is run in the absence of radical trap is consistent with mechanism depicted in Scheme 4. Indeed, both the O-substitution product and 4-nitrobenzaldehyde have to built up to a sufficient extent before the formation of the pinacol starts and these conditions are never fulfilled in the absence of trap since the reaction is then mostly driven toward the $S_{RN}1$ pathway.

At this stage, despite the complication created by the formation of the pinacol in the presence of a radical trap, we may conclude, for the sake of the following discussion, that the kinetics of the reaction are governed by the competing formation of the C-substitution product according to a $S_{RN}1$

(14) (a) With such a fast reaction, the time required for mixing the reactants ceases to be negligible compared to the half-reaction time; 1 min is thus an upper limit. (b) The pK_a s of 2-nitropropane and water in DMSO are 16.9 and 31.2, respectively.[14c] (c) Bordwell, F. G. *Acc. Chem. Res.* **1988**, *21*, 456.

(15) 4-nitrobenzaldehyde exhibits a reversible wave at scan rates as low as 0.1 V/s corresponding to a standard potential of −0.85 V vs SCE. The electron transfer from the 2-nitropropanate ion to 4-nitrobenzaldehyde is thus largely endergonic, with standard free energy of reaction equal to 0.927 eV, corresponding to an equilibrium constant of 1.3×10^{-16}. If the dimerization step is under diffusion control, the rate constant for the pinacol formation would be 3×10^{-6} $M^{-1}s^{-1}$. Because of Coulombic repulsion, the dimerization of the two anion radicals should be somewhat below the diffusion limit. It follows that the preceding estimate is an upper limit.

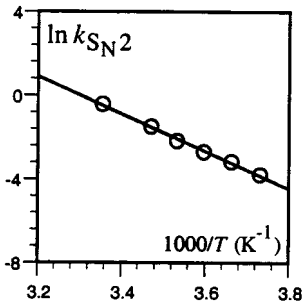

Figure 2. Reaction of 4-nitrobenzyl chloride (2 mM) with tetramethylammonium 2-nitropropanate (4 mM) in the presence of di-*tert*-butyl nitroxide (1.62 mM). Variation of the O-substitution S_N2 rate constant with temperature. The equation of the straight line is: $k_{S_N2} = \ln A - E_A/RT$ with $\ln(A/M^{-1}\ s^{-1}) = 29.48$ and $E_A = 0.77$ eV.

mechanism and of the O-substitution product according to a S_N2 mechanism. The first process is faster than the second but not much faster (the half-reaction times are 1 and 4.8 min respectively).

Figure 2 shows the Arrhenius plot for the S_N2 O-substitution reaction that we have derived from experiments run at several temperatures in the presence of the same radical trap present in sufficient concentration to quench all the $S_{RN}1$ reactivity. The value thus obtained for the activation energy will be used in the discussion of a possible mechanism bifurcation from the S_N2 to the dissociative electron-transfer pathways (section 6).

In the following sections, we will try successively the various possible initiation mechanisms. In each case, the predicted kinetics and product distribution will be compared to the experimental data. The product distribution indeed appears as particularly discriminating in this respect. Repeated experiments indicated that the uncertainty on the yields is ±1%. With each initiation mechanism that will be examined, it is important to estimate the uncertainties affecting the rate constant data and, from them, to determine the resulting accuracy of the simulated product distribution to see whether a definite conclusion can be drawn. In most cases, the hypothesized mechanism will not lead to a fast enough initiation as attested by the simulated product distribution being less in favor of the C-substitution product (or, equivalently more in favor of the O-substitution product) than observed experimentally. The analysis will therefore proceed according to the following a fortiori type of argument. The slowest step of the propagation loop, k_{prop}, will first be identified and the range of uncertainty on its determination, Δk_{prop}, estimated. The error on the termination steps may be estimated as ±20%. Thus: $\Delta k_{term} = 0.2\ k_{term}$. The O-substitution S_N2 rate constant can similarly be bracketed after estimation of the range of error, Δk_{S_N2}. We obtain an upper limit of the predicted C-substitution yield by performing the simulation de novo for $k_{prop} + \Delta k_{prop}$, $k_{term} - \Delta k_{term}$, and $k_{S_N2} - \Delta k_{S_N2}$. Observing that the predicted yield thus obtained is clearly below the experimental yield rules out the tested mechanism.

2. Kinetics of the Propagation and Termination Steps. One of the three steps of the propagation loop (Scheme 1) is the cleavage of the anion radical of 4-nitrobenzyl chloride. Its rate constant, k_c, was measured by a combination of cyclic voltammetric and redox catalysis experiments. The cyclic voltammetric wave at which the reductive cleavage takes place remains irreversible at all investigated scan rates. The reduction is of the stepwise type and the wave is governed by the kinetics of both the electron transfer and cleavage steps. The variation of the peak potential with the scan rate thus provides two relationships between three parameters, namely, the standard potential for the formation of the anion radical, $E^0_{RX/RX^{\bullet-}}$, the standard rate constant for electron transfer, $k^S_{RX/RX^{\bullet-}}$ and the cleavage rate constant k_c. Redox catalysis experiments using duroquinone as the mediator provide a third relationship between the three parameters. The values derived from these three relationships are listed in Table 1 and details on their derivation are given in Appendix 1.

Table 1. Reaction of 4-Nitrobenzyl Chloride with the 2-Nitropropanate Ion[a] (Pertinent Rate Constants)[b]

half-reaction time	$t_{1/2} \approx 1$ min
product distribution	C-substitution: (93 ± 1)%, O-substitution: (7 ± 1)%
standard potentials[c]	$E^0_{RX/RX^{\bullet-}} = -1.094$, $E^0_{RNu/RNu^{\bullet-}} = -1.127$ V vs SCE
propagation	$k_c = 5.7 \times 10^6$,[d] $6.3 \times 10^7 < k_{Nu} < 11.3 \times 10^7$ $k_p = 1.1 \times 10^9$, $k_{-p} = 3.2 \times 10^8$
termination[e]	$k_{d1} = 2.6 \times 10^9$, $k_{d2} = 10^9$, $k_{rc} = 1.3 \times 10^9$, $k_{r1} = k_{r2} = 2 \times 10^{10}$
S_N2 substitution	$0.6 \le k_{S_N2} \le 0.75$

[a] Reaction of 2 mM 4-nitrobenzyl chloride with 4 mM tetramethylammonium 2-nitropropanate in CH_3CN at 20 °C. [b] In $M^{-1}s^{-1}$ unless otherwise stated. [c] In V vs SCE. [d] s^{-1}. [e] The various rate constants are defined as follows. k_{d1}, k_{d2}: self-coupling between two 4-nitrobenzyl and two 2-nitropropyl radicals, respectively. k_{rc}: mixed coupling. k_{r1}, k_{r2}: reduction of the 4-nitrobenzyl radical by $RX^{\bullet-}$ and $RNu^{\bullet-}$ respectively.

The standard potential for the formation of the C-substituted product, $E^0_{RNu/RNu^{\bullet-}}$ (Table 1), was derived from its reversible cyclic voltammetric wave. It follows that the *electron transfer from RNu$^{\bullet-}$ to RX in the propagation loop* has a standard free energy of reaction equal to

$$E^0_{RNu/RNu^{\bullet-}} - E^0_{RX/RX^{\bullet-}} = -0.044\ V$$

We hence find the rate constant values, k_p and k_{-p}, reported in Table 1, assuming that the self-exchange rate constant for each of the two couples is the same as for the dinitrobenzene/dinitrobenzene anion radical couple, $6 \times 10^8\ M^{-1}\ s^{-1}$.[16]

Unlike the 4-nitrocumyl case,[3] *the rate constant*, k_{Nu}, for the *coupling of the 4-nitrobenzyl radical with the 2-nitropropanate ion* could be obtained at 20 °C neither by direct cyclic voltammetry nor by redox catalysis because, at this temperature, the "thermal" $S_{RN}1$ reaction is too fast. The ratio k_{Nu}/k_c was derived from the decrease of the cyclic voltammetric peak current upon addition of the nucleophile at temperatures low enough to allow a reliable measurement. The bracketing values reported in Table 1 were obtained by extrapolation at room temperature of the resulting Arrhenius plot (see Appendix 2 for details).[17] Particular care was taken to estimate the range of uncertainty in this case for this reaction is the slowest of the propagation steps for the concentrations of reactants used in the experiment.

(16) Kojima, H.; Bard, A. J. *J. Am. Chem. Soc.* **1975**, *117*, 2120.

(17) Although this is not the main thrust of the present study, we may note en passant that the cleavage rate constant is larger in the cumyl than in the benzyl case while the opposite is true for the reaction of the two radicals with the 2-nitropropanate ion. 4-nitrocumyl: $k_c = 4.0 \times 10^7\ s^{-1}$, $k_{Nu} = 1.2 \times 10^6\ M^{-1}\ s^{-1}$, $E^0_{RX/RX^{\bullet-}} = -1.120$, $E^0_{RNu/RNu^{\bullet-}} = 1.120$ V vs SCE, $D_{RX\rightarrow R^{\bullet}+X^{\bullet}} = 2.575$ eV; 4-nitrobenzyl; $k_c = 5.7 \times 10^6\ s^{-1}$, $k_{Nu} = 8.2 \times 10^7\ M^{-1}\ s^{-1}$, $E^0_{RX/RX^{\bullet-}} = -1.094$, $E^0_{RNu/RNu^{\bullet-}} = 1.127$ V vs SCE, $D_{RX\rightarrow R^{\bullet}+X^{\bullet}} = 2.725$ eV. The standard free energies of the two reactions are:[2j] $\Delta G^0_{RX\rightarrow R^{\bullet}+X^-} = D_{RX\rightarrow R^{\bullet}+X^{\bullet}} + E^0_{RX/RX^{\bullet-}} - E^0_{X^{\bullet}/X^-} - T\Delta S_{RX\rightarrow R^{\bullet}+X^{\bullet}}$ and: $\Delta G^0_{R^{\bullet}+Nu^-\rightarrow RNu} = -D_{RNu\rightarrow R^{\bullet}+Nu^{\bullet}} - E^0_{RNu/RNu^{\bullet-}} + E^0_{Nu^{\bullet}/Nu^-} + T\Delta S_{RNu\rightarrow R^{\bullet}+Nu^{\bullet}}$, respectively. The decrease of the cleavage rate constant from cumyl to benzyl appears to be mainly caused by the increase of the bond dissociation energy in RX, which results from the fact that the tertiary cumyl radical is more stable than the primary benzyl radical. Likewise, the acceleration of the reaction from cumyl to benzyl is mostly a consequence of the increase of the bond dissociation energy in RNu for the same reasons as in RX, plus a destabilizing steric effect in the case of the coupling of the 4-nitrocumyl radical with the 2-nitropropanate ion.

The same care was also exerted in the determination of the rate constant of the S_N2 O-substitution as depicted in the preceding section (see Appendix 3 for details on the determination of the range of uncertainty).

The values selected for the rate constants for the various radical coupling *termination* steps were based on the dimerization rate constant of the benzyl radical, 2.6×10^9 M^{-1} s^{-1},[18] leading to the values reported in Table 1. The reduction of the radical $R^\bullet$ by the anion radicals $RX^{\bullet-}$ and $RNu^{\bullet-}$ are both very downhill reactions with a driving force of the order of 0.8 eV and may thus be considered as being under diffusion control.

3. Outersphere Electron Transfer Followed by Bond Cleavage? We may now simulate[19] the experimental data for this mechanism. We need an estimate of the forward and backward rate constants of the outersphere electron transfer, k_i and k_{-i}. They may be derived from equations (1−3), which depict the combination of activation and diffusion controls.[6b,20]

$$\frac{1}{k_i} = \frac{1}{k_{dif}} + \frac{1}{k_{act}} + \frac{1}{k_{dif}\exp\left[\frac{F}{RT}(E^0_{RX/RX^{\bullet-}} - E^0_{Nu/Nu^{\bullet-}})\right]} \quad (1)$$

$$\frac{k_i}{k_{-i}} = \exp\left[\frac{F}{RT}(E^0_{RX/RX^{\bullet-}} - E^0_{Nu/Nu^{\bullet-}})\right] \quad (2)$$

$$k_{act} = Z^{hom}\exp\left[-\frac{F}{RT}\frac{\lambda}{4}\left(1 + \frac{E^0_{Nu/Nu^{\bullet-}} - E^0_{RX/RX^{\bullet-}}}{\lambda}\right)^2\right] \quad (3)$$

Z^{hom} is the bimolecular encounter frequency and k_{dif}, the bimolecular diffusion limit. In view of the very low driving force, only the two last terms in the right-hand side of eq 1 are significant. The total reorganization energy, noted λ, is the sum of the solvent and intramolecular reorganization energies, λ_0 and λ_i. λ_0 is estimated according to the Marcus−Hush model[20] while λ_i is derived from the standard rate constants for the electrochemical reduction of 4-nitrobenzyl chloride (see Appendix 1) and the oxidation of the 2-nitropropanate ion.[3] The details of this derivation and of the estimation of Z^{hom} are given in Appendix 4. We thus find: $k_i = 2.9 \times 10^{-10}$ M^{-1} s^{-1} and $k_{-i} = 1.8 \times 10^{10}$ M^{-1} s^{-1}.

We dispose now of all the necessary ingredients for simulating the distribution of products and the half-reaction time. It is seen (Table 2) that the predicted yield in C-substitution product, 2%, is much lower than the experimental yield pointing to the conclusion that outersphere electron transfer between the 2-nitropropanate and 4-nitrobenzyl chloride is not a viable initiation step for the $S_{RN}1$ reaction. This conclusion is confirmed by the observation that the predicted half-reaction time, 4.75 min is only very slightly shorter than the half-reaction time of the S_N2 O-substitution, 4.8 min, in line with the very small amount of $S_{RN}1$ product predicted to be formed according to this initiation mechanism.

It is interesting to estimate the effect that the uncertainties on the rate constants of the various steps involved may have on the simulation of the product distribution. We thus take, as rate constant values, the limits of each uncertainty range appropriate for maximizing the C-substitution yield, namely $k_{Nu} = 6.3 \times 10^7$ (since they are not rate determining, the values of the rate constants of the two other propagation steps are kept the same as before), $k_{S_N2} = 0.6$, $k_i = 4.2 \times 10^{-10}$, $k_{-i} = 1.3 \times 10^{10}$ M^{-1} s^{-1} and for the termination steps, values which are 20% lower than the values we used earlier. The predicted yield (Table 2) is thus found equal to 4%, again much smaller than the experimental yield, therefore confirming the above conclusion.

Table 2. Simulation of Product Distribution and Reaction Kinetics for Each Initiation Mechanism[a]

	C-substitution yield (%)
experimental	93 ± 1
outersphere electron transfer followed by bond cleavage	2 (<4)
dissociative electron transfer with negligible interaction between caged fragments	4 (<6.5)
initiation by the oximate	24[b]
produced in the S_N2 O-substitution reaction	4.5[c]
initiation through mechanism bifurcation in the S_N2 O-substitution reaction	7 (<9)
dissociative electron transfer with 105 meV interaction between caged fragments	93

[a] Same conditions as in Figure 1a unless otherwise stated. [b] In the presence of 4 mM 2-nitropropane. [c] In the presence of 275 mM 2-nitropropane.

4. Dissociative Electron Transfer with Negligible Interactions between Caged Fragments? Since the reaction is endowed with a very poor driving force, it is conceivable that the mechanism has shifted to dissociative electron transfer as was indeed the case with 4-nitrocumyl chloride.[3] We may thus examine whether dissociative electron transfer with negligible interaction between the caged fragments, leading directly to the 4-nitrobenzyl radical (Scheme 2), offers a viable alternative to the outersphere mechanism. The initiation step is now irreversible, and its rate constant, k_i', may be estimated according to the same strategy as already used successfully in the cumyl case,[3] i.e.

$$k_i' = Z^{hom}\exp\left[-\frac{F}{RT}\frac{\lambda'}{4}\left(1 + \frac{E^0_{Nu^\bullet/Nu^-} - E^0_{RX/R^\bullet+X^-}}{\lambda'}\right)^2\right] \quad (4)$$

with $\lambda' = D + \lambda_0' + \lambda_i'$, where D is the R−X bond dissociation energy. For λ_0', the solvent reorganization energy, we may take the same value, 0.505 eV as already used in the outersphere case. λ_i' is the intramolecular reorganization energy besides the reorganization energy pertaining to the cleavage of the R−X bond. It is equal to the electrochemical intramolecular reorganization energy for the oxidation of Nu^-, 0.296 eV.

The standard potential for the dissociative electron transfer may be expressed as

$$E^0_{RX/R^\bullet+X^-} = -D + E^0_{X^\bullet/X^-} + T(S_{R^\bullet} + S_{X^\bullet} - S_{RX})$$

$E^0_{X^\bullet/X^-}$ is equal to 1.89 V vs SCE in acetonitrile.[21] D and the standard molar entropies were estimated by means of B3LYP density functional quantum chemical calculations (see the Methodology section): $D = 2.725$ eV, [22] $S_{R^\bullet} = 3.65$, $S_{X^\bullet} = 1.38$, $S_{RX} = 4.06$ meV/K. We thus find $E^0_{RX/R^\bullet+X^-} = -0.549$ V vs SCE. It follows from eq 4 that $k_i' = 8.6 \times 10^{-10}$ M^{-1} s^{-1}.

Simulation using these values (Table 2) predicts a C-substitution yield, 4%, which is again much lower than the

(18) Lehni, M.; Schuh, H.-H.; Fischer, H. *Int. J. Chem. Kinet*. **1979**, *11*, 705.

(19) Braun, W.; Herron, J. T.; Kahaner, D. K. *Int. J. Chem. Kinet*. **1988**, *20*, 51.

(20) (a) Marcus, R. A. *J. Chem. Phys*. **1956**, *24*, 4966. (b) Hush, N. S. *J. Chem. Phys*. **1958**, *28*, 962. (c) Marcus, R. A. In *Special Topics in Electrochemistry*; Rock, P. A., Ed.; Elsevier: New York, 1977; pp 161−179.

(21) Andrieux, C. P.; Differding, E.; Robert, M.; Savéant, J.-M. *J. Am. Chem. Soc*. **1993**, *115*, 6592.

experimental yield. We also observe that the value predicted for the half-reaction time, 4.7 min is only very slightly shorter than the half-reaction time of the S_N2 O-substitution, 4.8 min, in line with the very small amount of $S_{RN}1$ product predicted to be formed according to this initiation mechanism. For estimating the effect of uncertainty on rate constants on the predicted yield we use the same values as in the preceding section for propagation and termination.

We may neglect the uncertainty on k_i' by reference to what has been observed in the cumyl case. The determination of k_i' was made in the cumyl case exactly as in the present case: the kinetic law was the same; the procedures for determining $E^0_{RX/R^{\bullet}+X^-}$, λ_0 and D were the same. In the cumyl case, the predicted efficiency of the $S_{RN}1$ reaction was slightly larger than the experimental data. It follows that if the value of k_i' we use here were in error, this error should lead to an overestimation of the predicted C-substitution yield which fits our a fortiori argument. The upper limit thus found, 6.5%, is again much lower than the experimental value (Table 2).

We thus reach the conclusion that, unlike the cumyl case, a dissociative electron transfer from the 2-nitropropanate ion to 4-nitrobenzyl chloride, with no interaction between caged fragments, is not a viable initiation step for this "thermal" $S_{RN}1$ reaction.

What are the differences between the two chlorides that may cause this difference in behavior? Three possible causes may be identified. The $S_{RN}1$ reaction competes with an S_N2 O-substitution reaction in the present case whereas this does not happen in the cumyl case. One consequence is the formation of the acetone oxime (Scheme 3), which can be converted into the oximate ion by reaction with the 2-nitropropanate ion. We have thus to examine whether the oximate ion thus formed could be a better electron-transfer initiator than the 2-nitropropanate ion. Another consequence of the occurrence of the S_N2 O-substitution reaction is the possibility of a faster formation of the radical through a mechanism bifurcation following the passage through the S_N2 transition state. The last possibility is that attractive interactions between caged fragments are more likely in the benzyl case than in the cumyl case for steric and electronic reasons. We examine now these three possibilities successively.

5. Initiation by the Oximate Ion Produced in the S_N2 O-Substitution Reaction? The initiation mechanism involving the oximate ion as electron donor is summarized in Scheme 5. The electron-donor properties of the oximate ions were derived from its irreversible cyclic voltammetric oxidation wave as detailed in Appendix 5. The standard potential of the oximate radical/ oximate ion, $E^0_{oxm^{\bullet}/oxm^-} = -0.49$ V vs SCE, makes it a better reducing agent than the 2-nitropropanate ion on thermodynamical grounds. Albeit endowed with a large intrinsic barrier, this is also true in terms of kinetics since (Appendix 5) $k''_i = 2.3 \times 10^{-3}$ and $k''_{-i} = 5.5 \times 10^7$ M^{-1} s^{-1}.[23] The oximate ion thus appears as a possible candidate for serving as electron donor

Scheme 5

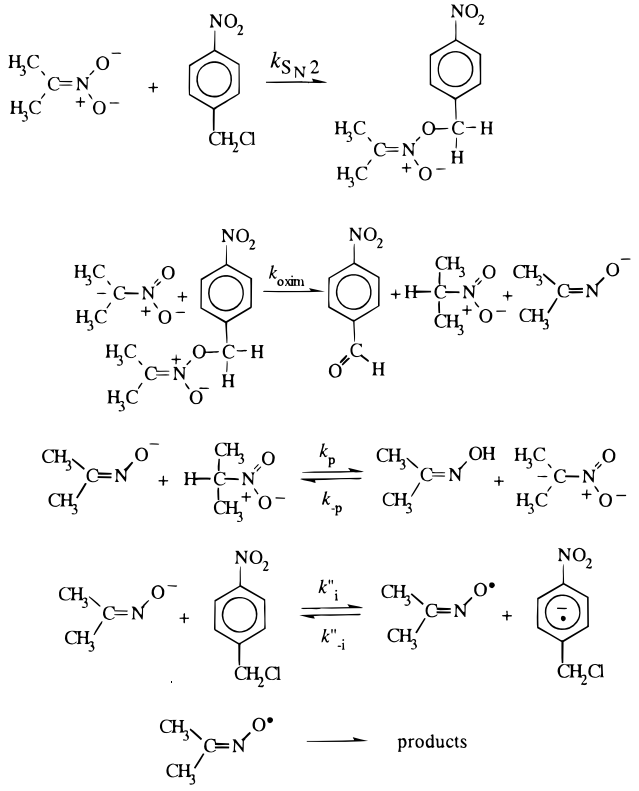

in the initiation. It has, however, to be formed in sufficient amounts in the conditions of the experiment depending on the efficiency of the first three steps in Scheme 5 for actually offering a viable alternative to initiation by the 2-nitropropanate ions.

We have estimated the standard free energies of the second and third reactions in Scheme 5 by density functional B3LYP calculations (see the Methodology section) and found -1.30 and 0.24 eV, respectively. The second reaction being strongly downhill, its rate constant is certainly much larger than k_{S_N2} (0.7 M^{-1} s^{-1}). The simulation is thus independent of the exact value taken for k_{oxim} (it was taken as equal to 10^2 M^{-1} s^{-1} in the following simulations). k_p and k_{-p} are not known separately (their ratio is 10^4). Several tests have showed that the simulations are independent of the exact value of k_p provided it is larger than 10^5 M^{-1} s^{-1}, corresponding to the protonation/deprotonation reaction being at equilibrium. In the following simulations we have taken $k_p = 10^7$ M^{-1} s^{-1}. The results (Table 2) show that electron transfer from the oximate ion is not a viable initiation step of the $S_{RN}1$ reaction. The various rate constants that have been used in the simulation are certainly approximate calling for a confirmation of this conclusion. This is provided by the effect of adding 2-nitropropane to the solution. As seen in Table 2, addition of 2-nitropropane is predicted to result in a significant decrease of the efficiency of the $S_{RN}1$ reaction (the yield in C-substitution product passes from 25 to 4.5% upon increasing the concentration of 2-nitropropane from 4 to 275 mM) as a result of the retrogradation of the proton exchange equilibrium in disfavor of the 2-nitropropanate ion. As noted earlier, the experimental yields are independent of the amount of 2-nitropropane present thus ruling out electron transfer from the oximate ion as a possible initiation step.

6. Initiation through Mechanism Bifurcation in the S_N2 O-Substitution Reaction? Recent ab initio computational work on small model systems has pointed to the importance that

(22) (a) For the BDE of 4-nitrobenzyl chloride, we find a slightly smaller value (2.725 eV) than in a recent publication (2.82 eV)[22b] and the difference with unsubstituted benzyl chloride is larger in our case (0.101 vs 0.070 eV). The cause of these discrepancies is likely due to the fact that we used the density functional B3LYP technique both for geometry optimization and energy calculation whereas the AM1 method was used in ref 22b for geometry optimization and B3LYP with a slightly different basis set energy calculations. (b) Pratt, D. A.; Wright, J. S.; Ingold, K. U. *J. Am. Chem. Soc.* **1999**, *121*, 4877.

(23) The standard free energy of reaction for the outersphere electron transfer, 0.6 eV, is still positive but much less than in the case of 4-nitropropanate. This is the reason that we have examined only the possibility of an outersphere electron transfer and not that of a dissociative electron transfer from the oximate ion.

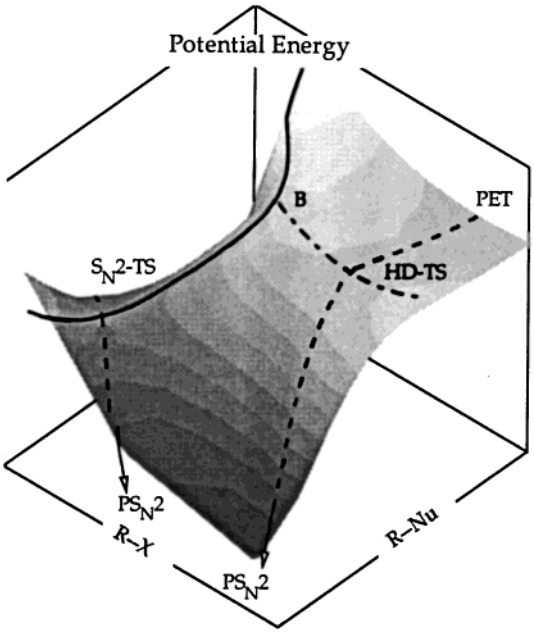

Figure 3. Product valleys in the S_N2 O-substitution reaction. The reactant system is behind and below the portion of surface shown. Full line: col separating the reactant and product valleys. Dashed lines: reaction paths for S_N2 and homolytic dissociation of the S_N2 product, respectively. Dashed/dotted line: ridge separating the ET plateau and the S_N2 valley. PS_N2, PET: S_N2 and PET products. S_N2-TS, HD-TS: S_N2 and homolytic dissociation transition states. B: bifurcation point.

mechanism bifurcation (for general analyses of mechanism bifurcation see refs 24) may have in product selection in the competition between S_N2 and dissociative electron transfer (ET) pathways.[7b,c] The competition involves two distinct pathways, a S_N2 and an ET pathway corresponding to two distinct transition states, which are connected to the S_N2 and ET products respectively by means of an intrinsic reaction coordinate path in each case. In addition, the ET products may also be obtained along the S_N2 pathway thanks to a bifurcation taking place at or past the col separating the reactant and product valleys. Two types of situations have been described.[7c,d] In one of these (as in the surface sketched in Figure 3), the ridge separating the S_N2 and ET valleys has its origin at a point, B, located on the col separating the reactant and product valleys. Another case is when the origin of the ridge is below the S_N2 saddle point. The system then remains for a while on the ridge before partitioning between the two valleys.

That the 4-nitrobenzyl chloride + 2-nitropropanate ion system belongs to the first category results from the fact that the energy of the ET products is higher than the S_N2 saddle point by 0.24 eV (Appendix 6). Since, point B is higher in energy than the ET products, it follows that point B stands higher than the S_N2 saddle point by more than 0.24 eV. The reverse of the homolytic dissociation of the O-substitution product may be assumed to proceed without significant activation barrier, as usually done when dealing with radical/radical couplings. Under these conditions, the ET product region on the potential energy surface is more of a plateau than of a valley (Figure 3). The result of this topology of the potential energy surface is, whatever its detailed characteristics, that the partitioning between the S_N2 and ET products is ultimately governed by the homolytic dissociation/radical coupling equilibrium.

We may thus simulate the experimental kinetics and product distribution according to the initiation mechanism depicted in Scheme 6. k_{-h} may be taken as equal to the diffusion limit, 2

Scheme 6

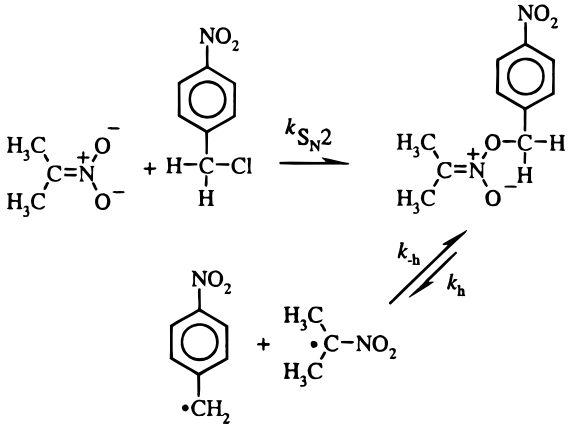

$\times 10^{10}$ $M^{-1}s^{-1}$. k_h may be derived from k_{-h}, after estimation of the standard free energy of homolytic dissociation, according to $k_h = k_{-h} \exp(-\Delta G_h^0/RT)$. We estimated that $\Delta G_h^0 = 1.27$ eV (see Appendix 6) and thus $k_h = 7 \times 10^{-12}$ s^{-1}. Entering these rate constants, together with $k_{S_N2} = 0.7$ M^{-1} s^{-1} into the simulation predict a C-substitution yield of 7% and a half-reaction time, 4.7 min, very close to the S_N2 half-reaction time. The upper limit obtained when taking into account the uncertainties on rate constants as in the preceding section still leads to a C-substitution yield (Table 2) much lower than observed experimentally, showing unambiguously that this initiation mechanism can also be ruled out.

7. Interaction between Caged Fragments in the Dissociative Electron-Transfer Initiation? Having exhausted the other mechanisms, we are thus left with the possibility that a small but significant interaction of the charge/dipole (+ induced dipole) exists between the 4-nitrobenzyl radical and chloride ion within the solvent cage. Such a situation is quite likely in the case of 4-nitrobenzyl chloride because of the electron-withdrawing character of the 4-nitro substituent and because the interaction is not counteracted by steric hindrance and the presence of the electron-donating α-methyl groups as in the case of 4-nitrocumyl chloride. In the description of the effect of bond stretching and cleavage, the purely repulsive Morse curve representing the product system should thus be replaced by a curve with an energy minimum corresponding to the attractive interaction, D_P, between the caged fragments (Figure 4).

Although the species at the shallow energy minimum is more of a cluster of interacting fragments than of a molecule, it might be viewed as a "σ anion radical" as opposed to the "π anion radical" represented in Figure 4 as $RX^{\bullet -}$. As represented in Figure 4, the principle of the distinction between the stepwise and concerted mechanism remains untouched. In the concerted case, the caged fragments form a loose intermediate, endowed with a shallow energy minimum, and ultimately diffuse apart. In the stepwise situation the reaction goes through an intermediate, the anion radical, which rapidly decomposes along a strongly downhill process giving rise to the same caged interacting fragments cluster before all fragments diffuse apart.

Despite the fact the energy minimum is the result of a charge dipole (and induced dipole) interaction rather than of the existence of a covalent bond, the product potential energy profile may be approximated by a Morse curve.[13a] Extension[13] of previous analyses,[2j] leads to equation describing the dynamics of this "sticky" dissociative electron transfer under the form of an activation-driving force relationship linking the activation free energy, $\Delta G^{\ddagger}$, to the standard free energy of the formation

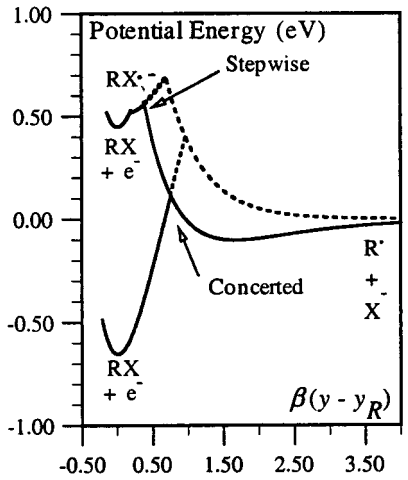

Figure 4. Reactant and product Morse curves showing the effect of a small interaction between caged fragments on the dynamics of the concerted and stepwise pathways (full lines) as compared to the absence of interaction (dotted line).

of separated fragments, $\Delta G°$, the bond dissociation energy of the cleaving bond, D, the interaction energy, D_P, the Marcus−Hush solvent reorganization energy, λ_0' and the intramolecular reorganization energy besides the reorganization energy pertaining to the cleavage of the R−X bond (equal to the electrochemical intramolecular reorganization energy for the oxidation of Nu^-), λ_i'.[25]

$$\Delta G^{\ddagger} \approx \frac{(\sqrt{D} - \sqrt{D_P})^2 + \lambda_0' + \lambda_i'}{4}\left[1 + \frac{\Delta G^0 - D_P}{(\sqrt{D} - \sqrt{D_P})^2 + \lambda_0' + \lambda_i'}\right]^2 \quad (5)$$

The initiation rate constant is given by

$$k_i' = Z^{hom} \exp\left(-\frac{F\Delta G^{\ddagger}}{RT}\right)$$

For Z^{hom}, $\Delta G^0 = E^0_{Nu^{\bullet}/Nu^-} - E^0_{RX/R^{\bullet}+X^-}$, D, λ_0', and λ_i', we take the same values as in section 4, namely, 3.9×10^{11} M^{-1} s^{-1}, 0.626, 2.725, 0.505, 0.296 eV, and we adjust D_P so as to reproduce the experimental C-substitution yield (Table 2). The value of D_P thus found is 0.105 eV, and the simulated half-reaction time is 30 s in line with the experimental estimate.[14a] With no interactions between the product fragments, $\Delta G^{\ddagger} = 1.22$ eV and $k_i' = 8.8 \times 10^{-10}$ M^{-1} s^{-1}; with a 0.105 eV attractive interaction, $\Delta G^{\ddagger} = 0.927$ eV and $k_i' = 8.3 \times 10^{-5}$ M^{-1} s^{-1}.

Similar effects, of a similar order of magnitude, transpire from the analysis of recent data. One such observation derives from recent results obtained in the electrochemical reduction of carbon tetrachloride.[13a] Kinetic characteristics of the electrochemical reduction of substituted benzyl halides may also be rationalized within the same framework. Whereas the electrochemical reduction of 4-nitrobenzyl bromide in DMF is, as seen earlier, clearly a stepwise reaction, a concerted mechanism is observed with unsubstituted benzyl and 4-cyanobenzyl bromides.[6d] The cyclic voltammetric peak potential of 4-cyanobenzyl bromide is significantly more positive than the cyclic voltammetric peak potential of benzyl bromide (by 250 mV at a scan rate of 0.1 V/s). It was inferred from these observations that the bond dissociation energy increases by 0.15 eV from the first to the second compound, in line with previous photoacoustic work,[26a] in which the substituent effect was regarded as concerning the starting molecule rather than the radical. However, further measurements using the same technique did not detect any substituent effect and the same conclusion was also reached in the gas phase by a low-pressure pyrolysis technique.[26b] Recent quantum chemical estimations[22b] concluded that there is a small substituent effect, namely, 0.07 eV, i.e., about half of the value derived from electrochemical experiments upon application of the classical dissociative electron transfer theory. These observations may be interpreted by a small attractive interaction between the caged product fragments that would be larger in the presence than in the absence of the cyano-substituent because of its electron-withdrawing character. An even larger similar effect is observed with phenacyl chloride and bromide as expected from the electron-withdrawing effect of the carbonyl group. The apparent bond dissociation energies derived from cyclic voltammetry[26c] are again significantly lower than the values derived from low-pressure pyrolysis.[26d]

It is remarkable that in all cases a measurable interaction between caged fragments appears only with molecules where strong electron withdrawing effects are present, thus reinforcing the charge/dipole (and induced dipole) between the anion leaving group and the radical making it strong enough to compete with the shielding effect of the polar solvent.

Conclusions

Although the reduction of 4-nitrobenzyl chloride by many electron donors occurs according to a stepwise mechanism involving the formation of the anion radical followed by bond cleavage, this is not the case with a weak reducing agent such as the 2-nitropropanate ion. The investigation of the reaction under such unfavorable thermodynamical conditions (standard free energy of the reaction of the order of 1.2 eV) is not feasible by conventional means. It is made possible by using $S_{RN}1$ amplification as a mechanistic tool, the formation of tiny amounts of 4-nitrobenzyl radicals being revealed and measured by the fact they trigger the formation of a C-substitution product whose yield and half-reaction time may be readily determined.

With such uphill reductive cleavages, it is expected that the mechanism can shift from stepwise to concerted as observed

(24) (a) Garrett, B. C.; Truhlar, D. G.; Wagner, A. F.; Dunning, T. H. *J. Chem. Phys.* **1983**, *78*, 4400. (b) Valtazanos, P.; Ruedenberg, K. *Theor. Chim. Acta* **1986**, *69*, 281. (c) Baker, J.; Gill, P. M. W. *J. Comput. Chem.* **1988**, *9*, 465. (d) Bosch, E.; Moreno, M.; Lluch J. M.; Bertran, J. *Chem. Phys. Lett.* **1989**, *1604*, 543. (e) Natanson, G. A.; Garrett, B. C.; Truong, T. N.; Joseph, T.; Truhlar, D. G. *J. Chem. Phys.* **1991**, *94*, 7875. (f) Schlegel, H. B. *J. Chem. Soc., Faraday Trans.* **1994**, *90*, 1569.

(25) Rigorously speaking the standard free energy term in eq 5 writes $\Delta G^0 - \Delta G^0_{sp}$ rather than $\Delta G^0 - D_P$, with $D_P - T\Delta S^0_{sp}$ is the difference between the standard free energies of the separated and the caged fragments. This relationship indicates that the effect of an interaction between the fragments in the product cluster is not merely described by the introduction of a work term. Such a work term appears under the form of ΔG^0_{sp}, but there is also a modification of the intrinsic barrier, D being replaced by $(\sqrt{D} - \sqrt{D_P})^2$.

(26) (a) Clark, K. B.; Wayner D. D. M. *J. Am. Chem. Soc.* **1991**, *113*, 9363. (b) Laarhoven, L. J. J.; Born, J. G. P.; Arends, I. W.; Mulder, P. *J. Chem. Soc., Perkin Trans. 2* **1997**, 2307. (c) Andrieux, C. P.; Savéant, J.-M.; Tallec, A.; Tardivel, R.; Tardy, C. *J. Am. Chem. Soc.* **1997**, *119*, 2420. (d) Dorrestijn, E.; Hemmink, S.; Hultsmaan, G.; Monnier, L.; Van Scheppingen, W.; Mulder, P. *Eur. J. Org. Chem.* **1999**, 607.

(27) (a) Amatore, C.; Chaussard, J.; Pinson, J.; Savéant, J.-M.; Thiébault, A. *J. Am. Chem. Soc.* **1979**, *101*, 6012. (b) Amatore, C.; Pinson, J.; Savéant, J.-M.; Thiébault, A. *J. Am. Chem. Soc.* **1982**, *104*, 817. (c) Amatore, C.; Oturan, M. A.; Pinson, J.; Savéant, J.-M.; Thiébault, A. *J. Am. Chem. Soc.* **1985**, *107*, 3451. (d) Amatore, C.; Savéant, J.-M.; Thiébault, A. *J. Electroanal. Chem.* **1979**, *103*, 303.

(28) Glasstone, S.; Laidler, K. J.; Eyring, H. *The Theory of Rate Processes*; McGraw-Hill: New York, 1941.

(29) Marcus, Y. *Ion Properties*; Marcel Dekker: New York, 1997.

with several electrochemical reactions and, in the homogeneous case, with the reaction of 4-nitrocumyl chloride with the very same 2-nitropropanate ion as electron donor. Careful simulation of the product distribution and half-reaction time showed unambiguously that, unlike the cumyl case, a dissociative electron transfer from the 2-nitropropanate ion to 4-nitrobenzyl chloride does not take place, at least if it is assumed that interactions between the 4-nitrobenzyl radical and the leaving chloride in the product solvent cage are negligible.

One important difference between the 4-nitrobenzyl and the 4-nitrocumyl chloride reactions is that S_N2 O-substitution takes place in the first case and not in the second. One consequence is the formation in the benzyl case of the oximate ion, which is a more potent reducing agent than the 2-nitropropanate ion. However, the formation of the oximate ion through deprotonation of the oxime by the 2-nitropropanate ion is not productive enough to make it a viable electron-transfer initiator.

It is also possible that a mechanism bifurcation following the S_N2 transition state and/or homolytic dissociation of the S_N2 product could produce an additional amount of 4-nitrobenzyl radicals entering the propagation loop. Although such possibility exist, they do not generate enough radicals to account for the observed formation of C-substitution product and half-reaction time.

We are thus left with one possibility, namely that the dissociative electron transfer be accelerated by a small but significant attractive interaction between the 4-nitrobenzyl radical and the leaving chloride in the solvent cage where they are formed. The magnitude, thus estimated, of this interaction, ca. 0.1 eV, seems quite reasonable as an outcome of the competition between two effects. On one hand, the interaction is weakened by the presence of the polar solvent. On the other, the interaction is strengthened by presence of a strong electron-withdrawing group which increases the positive charge on the reacting carbon and is not thwarted, as in the cumyl case by the steric and electron effect of the two methyl groups on the reacting carbon. This conclusion also matches observations that have been made in electrochemical reductions in similarly polar solvents, that of CCl_4 and also of other benzyl halides and of phenacyl halides. The example 4-nitrobenzyl chloride appears as the first example of the influence of an interaction between caged fragments on the dynamics of an homogeneous dissociative electron transfer reaction. It must be emphasized that the detection of this effect could be achieved only because $S_{RN}1$ amplification allowed the investigation of the electron-transfer reaction under much poorer driving forces than usually available. Indeed, on one hand, the presence of the NO_2 group is a favorable factor for a sizable interaction to be observed, but, on the other, the very presence of the NO_2 group makes the reductive cleavage follow a stepwise rather than a concerted mechanism under usual driving force conditions.

Another outcome of the study is that we now understand, after a long delay, why and how the first discovered $S_{RN}1$ reaction works with such a poor electron-donor initiator.

We hope that the strategy of using kinetic amplification by a chain process will receive further applications, noting that the $S_{RN}1$ reaction is not the only chain process one may think of to be exploited as a tool for investigating electron-transfer reactions under unusual thermodynamic conditions.

Experimental Section

Chemicals. Acetonitrile (Merck Uvasol), the supporting electrolyte NEt_4BF_4 (Fluka, puriss), 2-nitropropane (Aldrich), 4-nitrobenzyl chloride (Aldrich), tetramethylammonium hydroxide pentahydrate (Aldrich), duroquinone (Fluka), di-*tert*-butyl nitroxide (Aldrich), 4-nitrobenzaldehyde (Aldrich), and acetone oxime (Aldrich) were used as received. The tetramethylammonium salt of 2-nitropropane was prepared directly in the reaction vessel as described earlier.[3]

Silica gel (MN Kiesegel 60, 70−230 mesh, Macherey-Nagel) was used for column chromatography. Analytical TLC was performed with 0.25 mm coated commercial plates (Macherey-Nagel, Polygram SIL G/UV_{254}). NMR spectra were taken in $CDCl_3$ and using TMS as the internal standard for ^1H (200 MHz);^{13}C NMR spectra were measured in $CDCl_3$ at 50 MHz with all protons decoupled, and the chemicals shifts are reported in ppm downfield of TMS. Melting points are uncorrected. A 25 cm Kromasil C18 column, using CH_3CN 50%−H_2O 50% as eluent (UV detection at 270 nm) was used for high-pressure liquid chromatography analysis.

Reactions of 4-Nitrobenzyl Chloride with Tetramethylammonium 2-Nitropropanate. Kinetic Studies. A 8 mM solution of tetramethylammonium 2-nitropropanate in acetonitrile was prepared as described elsewhere.[3] It was transferred, in the dark, under argon, in an equal volume of a continuously stirred deoxygenated solution of 4-nitrobenzyl chloride (4 mM) in acetonitrile. The transfer duration was less than 1 min. At successive times, 100 μL of the solution were sampled and immediately added to a 100 μL of an acetonitrile solution of acetic acid in order to quench the unreacted nucleophile. The resulting solution was then analyzed by HPLC.

The same reaction procedure was followed in the experiments where the reaction was carried in the presence of di-*tert*-butyl nitroxide.

In all cases, the samples were analyzed by a high-pressure liquid chromatography (Gilson instrument) with a UV detection at 270 nm. The concentrations of each product were determined by comparison with authentic samples. M. Crozet kindly provided a sample of the C-substitution product.[1a]

Identification of the Reaction Products in the Presence of Di-*tert*-butyl Nitroxide. A 100 mL solution of the nucleophile (92 mM) was prepared as described elsewhere.[3] It was transferred, in the dark, under argon, in a 100 mL deoxygenated solution of 4-nitrobenzyl chloride (46 mM) and di-*tert*-butyl nitroxide (10 mM) in acetonitrile. The solution was stirred during 1 h. HPLC analysis showed that 4-nitrobenzyl chloride had completely disappeared and that three reaction products had been formed. One of them was identified as 4-nitrobenzaldehyde by comparison with an authentic sample. The second results from the reaction of 4-nitrobenzaldehyde with the nucleophile as checked independently. The third product was identified by means of the following procedure. A 900 μL portion of acetic acid was added to the solution. After solvent evaporation and addition of CH_2Cl_2, the remaining white solid (most probably NMe_4Cl) was removed by filtration. Evaporation of the CH_2Cl_2 solution left a crude material that was shown by HPLC to contain the three products. The unknown product was separated by silica gel chromatography (Et_2O/hexane 65:35). This gave a solid that was dried under vacuum and identified as the 1,2-bis-(4-nitrophenyl)-ethane-1,2-diol.

1,2-Bis(4-nitrophenyl)ethane-1,2-diol: mp 170 °C (powder); ^1H NMR δ 4.5 (s, 2H, CH) δ 7.4 (m, 4H, H-arom) δ 8.1 (m, 4H, H-arom); ^{13}C NMR δ 59.0, 123.3, 127.4, 140.63, 147.57 MS (CI,CH_4) 305 ($M + H^+$). Anal. Calcd for $C_{14}H_{12}N_2O_6$: C, 55.26; H, 3.95; N, 9.21. Found: C, 55.50; H, 3.93; N, 9.26.

Cyclic Voltammetry. The working electrode was a 3 mm-diameter glassy carbon disk carefully polished and ultrasonically rinsed in ethanol before use. The counter-electrode was a platinum wire and the reference electrode an aqueous SCE electrode. The potentiostat, equipped with a positive feedback compensation and current measurer was the same as previously described.[30] For the low-temperature experiments, the cell was thermostated by circulating isopropyl alcohol and the reference electrode was maintained at 20 °C (the bridge containing the reference electrode was equipped with a double-wall jacket allowing circulation of water).

The experiments devised for determining the rate constant of coupling between the 4-nitrobenzyl radical and the 2-nitropropanate ion by direct cyclic voltammetry were carried out at low temperature and rapidly before the thermal reaction has time to take place to a significant extent. The following procedure was applied in this purpose.

(30) Garreau, D.; Savéant, J.-M. *J. Electroanal. Chem.* **1972**, *35*, 309.

A 10 mL solution of twice the final concentration of 4-nitrobenzyl chloride is prepared and shared in two 5 mL portions. Mixing one of these portions with 5 mL of a solution of pure supporting electrolyte and recording of the voltammogram allows the determination of the peak current in the absence of nucleophile, i_p^0. Rapid mixing, within a few seconds, of the second of these portions with a 5 mL of a solution containing twice the final concentration of the nucleophile (both solutions are thermostated at the same temperature) and immediate recording of the voltammogram allows the determination of the peak current in the presence of nucleophile, i_p.

Methodology for Quantum Chemical Calculations

All calculations were carried out with the Gaussian 94 package[31] using the B3LYP density functional method[32] with a 6-31G*[33] basis set. The geometries and electronic energies were calculated by full optimization of the conformations. The enthalpies and molar entropies were obtained after calculation of the frequencies. These values were corrected by a scaling factor (0.9804) applied to the zero-point energies and thermal energy corrections.[34]

The radii of the equivalent spheres of the various species of interest were obtained by means of a volume calculation on the optimized geometries, meaning the volume inside a contour of 0.001 electrons/bohr^3 density.

Appendix 1. Determination of $E^0_{RX/RX^{\bullet -}}$, $E^0_{RNu/RNu^{\bullet -}}$, $k^S_{RX/RX^{\bullet -}}$, and k_c by means of cyclic voltammetry and redox catalysis

The first wave in the cyclic voltammograms of 4-nitrobenzyl chloride (Figure 5) is a two-electron irreversible wave at which reductive cleavage and further reduction take place according to Scheme 7 to yield 4-nitrotoluene, which exhibits a one-electron reversible wave at a more negative potential.

The variation of the irreversible peak potential, E_p, with the scan rate, v, is shown in Figure 5b. The value of the peak potential at each scan rate is a function of the two following parameters[5]

$$E^0_{RX/RX^{\bullet -}} + \frac{RT}{2F}\ln\left(\frac{RT}{F}\frac{k_c}{v}\right)$$

$$\left(\text{or, alternatively, } E^0_{RX/RX^{\bullet -}} + \frac{2RT}{F}\ln\left[k^S_{RX/RX^{\bullet -}}\left(\frac{RT}{Fv D_i}\right)^{1/2}\right]\right)$$

and

$$\left(\frac{RT}{Fv}\right)^{1/2}\frac{(k^S_{RX/RX^{\bullet -}})}{k_c^{1/2}D_i}$$

(D_i is the diffusion coefficient). The above expressions assume that the transfer coefficient is equal to 0.5. The validity of this assumption derives from the fact that, as seen later on, the peak potential and the standard potential are close one to the other. The data in Figure 5b thus provide two relationships between the three parameters $E^0_{RX/RX^{\bullet -}}$, k_c, and $k^S_{RX/RX^{\bullet -}}$. A third relationship, namely

$$E^0_{RX/RX^{\bullet -}} + \frac{2RT}{F}\ln k_c = -0.695 \text{ V vs SCE} \qquad (6)$$

is obtained from redox catalysis (see below). It follows, taking $D_i = 10^{-5}$ cm^2 s^{-1}, that $E^0_{RX/RX^{\bullet -}} = -1.094$ V vs SCE, $k_c = 5.7 \times 10^6$ s^{-1} and $k^S_{RX/RX^{\bullet -}} = 0.98$ cm s^{-1}. The preceding analysis was carried out in the framework of an ECE mechanism rather than a DISP mechanism[5] as justified by the value of k_c thus found. Indeed, the competition between the two mechanisms is governed by the parameter:[5b] $(Fv/RT)^{1/2}\, k_{disp}C^0/k_c^{3/2}$ (C^0 is the bulk concentration of substrate). The DISP solution electron transfer is a very downhill reaction (standard free energy of ca. - 0.7 eV) and thus $k_{disp} = k_{dif} = 2 \times 10^{10}$ M^{-1} s^{-1}. It follows that, within the range of scan rates we explored (0.1−20 V/s), the above parameter ranges from 4×10^{-3} to 8×10^{-2}, i.e., values that are much in favor of the ECE pathway.

The *redox catalysis*[5b,c] experiments were carried out with duroquinone as the mediator (standard potential: − 0.80 vs SCE) and analyzed in the framework of Scheme 8. As seen in Figure 6a, i_p/i_p^0 is almost constant with the variation of the concentration of the mediator, C_Q^0, for a constant value of the excess factor C_{RX}^0/C_Q^0. This behavior is characteristic of a situation where the cleavage reaction is the rate-determining step of the catalytic process with the electron-transfer acting as a preequilibrium. It should also be taken into account that the coupling of the R$^\bullet$ radical with the anion radical of the catalyst (rate constant: k_{add}) counteracts the catalytic process. This is the reason that i_p/i_p^0 is not exactly constant with the variation of the concentration of the mediator. i_p/i_p^0 is thus a function of the

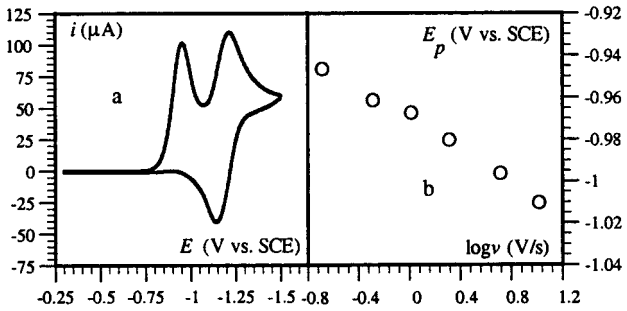

Figure 5. (a) Cyclic voltammetry of 4-nitrobenzyl chloride (2 mM) in CH_3CN + 0.1 M Et_4NBF_4 at 0.2 V/s. (b) Variation of the peak potential of the first cathodic wave with the scan rate.

Scheme 7. Reaction Scheme for the Cyclic Voltammetric Reduction of 4-Nitrobenzyl Chloride

1st 2e irreversible cathodic wave

$$RX + e^- \rightleftharpoons RX^{\bullet -}$$

$$RX^{\bullet -} \xrightarrow{k_c} R^\bullet + X^-$$

$$R^\bullet + e^- \rightleftharpoons R^- \quad \text{(ECE)}$$

and/or:

$$R^\bullet + RX^{\bullet -} \rightleftharpoons R^- + RX \quad \text{(DISP)}$$

$$R^- + H^+ \xrightarrow{k_{H^+}} RH$$

2nd 1e reversible cathodic wave

$$RH + e^- \rightleftharpoons RH^{\bullet -}$$

(31) Frisch, M. J.; Trucks, G. W.; Schlegel, H. B.; Gill, P. M. W.; Johnson, B. G.; Robb, M. A.; Cheeseman, J. R.; Keith, T.; Petersson, G. A.; Montgomery, J. A.; Raghavachari, K.; Al-Laham, M. A.; Zakrzewski, V. G.; Ortiz, J. V.; Foresman, J. B.; Cioslowski, J.; Stefanov, B. B.; Nanayakkara, A.; Challacombe, M.; Peng, C. Y.; Ayala, P. Y.; Chen, W.; Wong, M. W.; Andres, J. L.; Replogle, A. S.; Gomperts, R.; Martin, R. L.; Fox, D. J.; Binkley, J. S.; Defrees, D. J.; Baker, J.; Stewart, J. P.; Head-Gordon, M.; Gonzalez, C.; Pople, J. A. *Gaussian 94*, Revision E.1; Gaussian, Inc.: Pittsburgh, PA, 1995.

(32) Becke, A. D. *J. Chem. Phys.* **1993**, *98*, 5648.

(33) Pople, J. A.; Nesbet, R. K. *J. Chem. Phys.* **1974**, *22*, 571.

(34) Foresman, J. B.; Frisch, A. *Exploring Chemistry with Electronic Structure Methods*; Gaussian Inc.: Pittsburgh, PA, 1996.

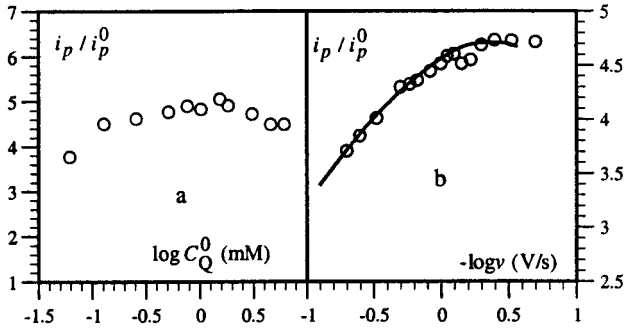

Figure 6. Redox catalysis of the reduction of 4-nitrobenzyl chloride by duroquinone in CH_3CN + 0.1 M Et_4NBF_4: (a) variation of the duroquinone peak current with the duroquinone concentration at 0.2 V/s; (b) variation of the duroquinone peak current with the scan rate for $C_Q^0 = 3$ mM. For both a and b, the ratio of the concentrations of substrate and mediator is constant and equal to 3.

Scheme 8

Redox Catalysis

$$Q \rightleftharpoons Q^{\bullet -}$$

$$Q^{\bullet -} + RX \underset{k_{-e}}{\overset{k_e}{\rightleftharpoons}} Q + RX^{\bullet -}$$

$$RX^{\bullet -} \xrightarrow{k_c} R^{\bullet} + X^-$$

$$R^{\bullet} + Q^{\bullet -} \xrightarrow{k_{red}} R^- + Q$$

$$R^{\bullet} + Q^{\bullet -} \xrightarrow{k_{add}} RQ^-$$

$$2R^{\bullet} \xrightarrow{k_d} \text{dimer and/or}$$

H-atom disproportionation products

$$R^- + H^+ \longrightarrow RH$$

$$RQ^- + H^+ \longrightarrow RQH$$

two dimensionless parameters

$$\rho = \frac{k_{red}}{k_{red} + k_{add}}$$

and

$$\frac{RT}{F}\frac{k_c}{v}\exp\left[\frac{F}{RT}(E^0_{RX/RX^{\bullet -}} - E^0_{Q/Q^{\bullet -}})\right]$$

The fitting of the experimental data points with the appropriate theoretical curve (solid line in Figure 6b) leads to eq 6 and to $\rho = 0.67$. The reduction of the R$^{\bullet}$ radical by the reduced form of the mediator has a driving force of ca. 0.5 eV. It may thus be considered to be at the diffusion limit ($k_{red} = k_{dif} = 2 \times 10^{10}$ M^{-1} s^{-1}) leading to $k_{add} = 10^{10}$ M^{-1} s^{-1}. (k_{add} is 2.5 times the value found for the 4-nitrocumyl radical in line with less steric hindrance to coupling in the first case than in the second).

Appendix 2. Determination of k_{Nu} by Means of Cyclic Voltammetry

The ratio k_{Nu}/k_c was derived from the decrease of the cyclic voltammetric peak current upon addition of the nucleophile at temperatures low enough to allow a reliable measurement (Figure 7). Under these conditions, the decrease of the peak current results from the electrochemically induced $S_{RN}1$ reaction

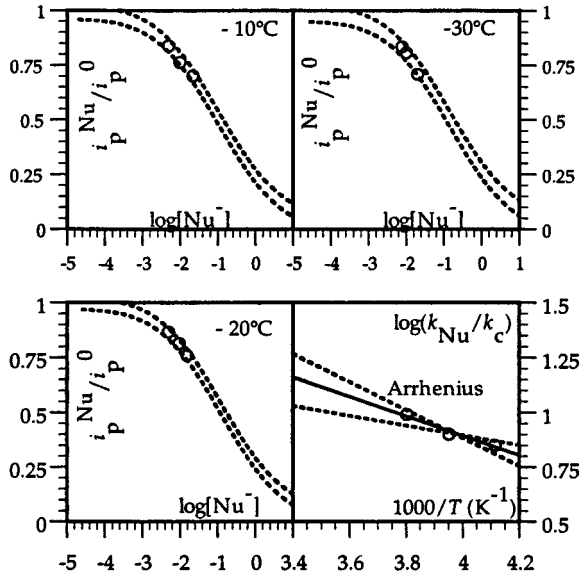

Figure 7. Decrease of the cyclic voltammetric peak current of 2 mM 4-nitrobenzyl chloride in CH_3CN + 0.1 M Et_4NBF_4 upon addition of tetramethylammonium 2-nitropropanate (concentrations in mM) at three temperatures (scan rate: 0.2 V/s) and ensuing Arrhenius plot.

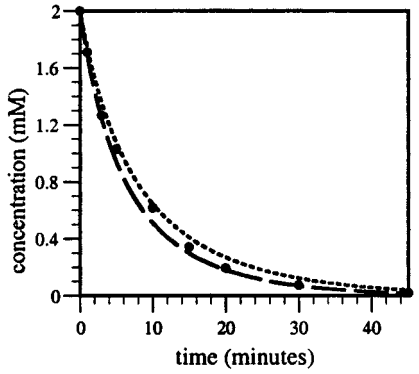

Figure 8. Bracketing of the S_N2 O-substitution rate constant. Variation of the concentration of 4-nitrobenzyl chloride with time upon addition of tetramethylammonium 2-nitropropanate (4 mM) in CH_3CN in the presence of di-*tert*-butyl nitroxide (1.62 mM). Temperature: 20 °C

and is a known function of the ratio k_{Nu}/k_c in the framework of an ECE mechanism. Fitting the experimental points with the appropriate working curve (Figure 7)[27] leads to the value of the rate constant ratio at each temperature and therefore to the Arrhenius plot represented in Figure 7. The value of the coupling rate constant is thus comprised between 6.3 and 11.3 $\times$ 10^7 M^{-1} s^{-1}.

Appendix 3. Kinetics of the S_N2 O-Substitution Reaction

Figure 8 shows the decay of the concentration of 4-nitrobenzyl chloride upon addition of 2-nitropropanate ion in the presence of a radical trap, di-*tert*-butyl nitroxide, at a concentration where the formation of the C-substitution product is completely suppressed. Bracketing of the experimental points by lower and upper limits led, after straightforward analysis of the second order decay curves, to 0.6 M^{-1} s^{-1} and $k_{S_N2} \leq 0.75$ M^{-1} s^{-1}.

Appendix 4. Kinetics of the Outersphere Electron Transfer RX + Nu−/RX•− + Nu•

In eq 3, Z^{hom} may be estimated as $Z^{hom} = (a_{Nu} + a_{RX})^2(8\pi RT/\mu)^{1/2} = 3.9 \times 10^{11}$ M^{-1}s^{-1} ($\mu = 58.16$ g is the reduced mass; $a_{Nu} = 3.88$ and $a_{RX} = 4.04$ Å are the radii of the equivalent

sphere derived after a quantum chemical calculation where the geometries were optimized using the B3LYP density functional method). The reorganization energy, λ, may be estimated as the sum of the solvent and intramolecular reorganization energies, λ_0 and λ_i. λ_0 is obtained from eq 7.[20]

$$\lambda_0 = 4\left(\frac{1}{2a_{\mathrm{Nu}}} + \frac{1}{2a_{\mathrm{RX}}} - \frac{1}{a_{\mathrm{Nu}} + 2a_{\mathrm{RX}}}\right) (\lambda_0 \text{ in eV}, a \text{ in Å}) \quad (7)$$

We thus find $\lambda_0 = 0.505$ eV. λ_i may be obtained from the electrochemical intramolecular reorganization energies for the two reactants according to eq 8.

$$\lambda_i = \lambda^{\mathrm{el}}_{i,\mathrm{Nu}^-} + \lambda^{\mathrm{el}}_{i,\mathrm{RX}} \quad (8)$$

The electrochemical reorganization energies may themselves be derived according to eq 9 from the previously determined electrochemical standard rate constants.[3]

$$k_{\mathrm{S}} = Z^{el} \exp\left[-\frac{F(\lambda^{\mathrm{el}}_0 + \lambda^{\mathrm{el}}_i)}{4RT}\right], Z^{\mathrm{el}} = \frac{RT}{2\pi M}\lambda^{\mathrm{el}}_0(\mathrm{eV}) = 3/a(\text{Å}) \quad (9)$$

(M: molar mass). We thus find $\lambda^{\mathrm{el}}_{0,\mathrm{Nu}^-} = 0.773$ eV, $\lambda^{\mathrm{el}}_{i,\mathrm{Nu}^-} = 0.296$ eV, $\lambda^{\mathrm{el}}_{0,\mathrm{RX}} = 0.743$ eV, $\lambda^{\mathrm{el}}_{i,\mathrm{RX}} = 0.128$ eV, $\lambda_i = 0.424$ eV. $\lambda = 0.929$ eV and therefore $k_i = 2.9 \times 10^{-10}$ M^{-1} s^{-1} and $k_{-i} = 1.8 \times 10^{10}$ M^{-1} s^{-1}. As expected for such a poor driving force of the forward electron-transfer step, the backward electron transfer step is practically under diffusion control. In other words, eqs 1 and 2 may be replaced by

$$k_{\mathrm{i}} = k_{\mathrm{dif}} \exp\left[\frac{F}{RT}(E^0_{\mathrm{RX/RX}^{\bullet -}} - E^0_{\mathrm{Nu}^{\bullet}/\mathrm{Nu}^-})\right]$$

and

$$k_{-i} = k_{\mathrm{diff}}$$

The uncertainty on k_{dif} may be estimated as ±20% and the error on each standard potential ±3 mV. A lower limit for k_{-i} is thus $0.80 \times 1.8 \times 10^{10} = 1.3 \times 10^{10}$ M^{-1} s^{-1} and an upper limit for k_i is $1.45 \times 2.9 \times 10^{-10} = 4.2 \times 10^{-10}$ M^{-1} s^{-1}.

5. Kinetics of the Outersphere Electron Transfer from the Oximate Ion

Oximate ions give rise to an irreversible one-electron cyclic voltammetric wave. At 0.1 V/s (in CH_3CN + 0.1 M Et_4NBF_4, at 20 °C with an oximate concentration of 2 mM) the peak potential is $E_{\mathrm{p}} = -0.111$ V vs SCE and the transfer coefficient derived from the peak width[5a,b] is $\alpha = 0.41$. From

$$\Delta G^{\ddagger} = \frac{\lambda^{\mathrm{el}}_0 + \lambda^{\mathrm{el}}_i}{4}\left[1 + \frac{E^0_{\mathrm{oxm}^{\bullet}/\mathrm{oxm}^-} - E_p}{\lambda^{\mathrm{el}}_0 + \lambda^{\mathrm{el}}_i}\right]^2$$

with

$$\Delta G^{\ddagger} = \frac{RT}{F}\left[\ln\left(Z^{\mathrm{el}}\sqrt{\frac{RT}{\alpha F \upsilon D}}\right) - 0.78\right]$$

($Z^{el} = \sqrt{RT/2\pi M} = 7.3 \times 10^3$ cm s^{-1} (M: molar mass) is the electrochemical collision frequency, υ is the scan rate, and D the diffusion coefficient) and

$$\alpha = \frac{1}{2}\left(1 + \frac{E^0_{\mathrm{oxm}^{\bullet}/\mathrm{oxm}^-} - E_{\mathrm{p}}}{\lambda^{\mathrm{el}}_0 + \lambda^{\mathrm{el}}_i}\right)$$

one obtains: $E^{\circ} = -0.49$ V vs SCE and $\lambda^{\mathrm{el}}_0 + \lambda^{\mathrm{el}}_i = 2.07$ eV. As discussed earlier,[3] λ^{el}_0 (eV) = $3/a$ (Å) (a, the radius of the equivalent hard sphere has been determined as equal to 3.8 Å by density functional B3LYP calculations). Thus, $\lambda^{\mathrm{el}}_i = 1.28$ eV and $\lambda^{\mathrm{el}}_0 = 0.79$ eV.

In view of the rather negative standard potential for the formation of the oximate ion, outersphere electron transfer to 4-nitrobenzyl chloride leading to the anion radical is faster than the dissociative electron transfer leading directly to the 4-nitrobenzyl radical and the chloride ion. The forward and backward rate constants of the new initiation step, k''_i and k''_{-i} are obtained from the following equation

$$\frac{1}{k''_i} = \frac{1}{k_{\mathrm{dif}}} + \frac{1}{k_{\mathrm{act}}} + \frac{1}{k_{dif}\exp\left[\frac{F}{RT}(E^0_{\mathrm{RX/RX}^{\bullet -}} - E^0_{\mathrm{oxm}^{\bullet}/\mathrm{oxm}^-})\right]}$$

with

$$k_{act} = Z^{\mathrm{hom}}\exp\left[-\frac{F}{RT}\frac{\lambda}{4}\left(1 + \frac{E^0_{\mathrm{RX/RX}^{\bullet -}} - E^0_{\mathrm{oxm}^{\bullet}/\mathrm{oxm}^-}}{\lambda}\right)\right]^2$$

$$Z^{\mathrm{hom}} = (a_{\mathrm{oxm}} + a_{\mathrm{RX}})^2\sqrt{8\pi RT/\mu} = 4.1 \times 10^{11}\ \mathrm{M}^{-1}\ \mathrm{s}^{-1}$$

(μ: reduced molar mass, a_{RX}, the radii of the equivalent hard sphere is equal to 4.04 Å) is the homogeneous collision frequency. The reorganization, λ, is the sum of three terms

$$\lambda = \lambda_0 + \lambda^{\mathrm{el}}_{i,\mathrm{RX}} + \lambda^{\mathrm{el}}_{i,\mathrm{oxm}}$$

λ_0, the solvent reorganization energy in the homogeneous cross-exchange electron transfer is given by the following equation

$$\lambda_0(\mathrm{eV}) = 4\left(\frac{1}{2a_{\mathrm{oxm}}} + \frac{1}{2a_{\mathrm{RX}}} - \frac{1}{a_{\mathrm{oxm}} + a_{\mathrm{RX}}}\right)$$

Since $a_{\mathrm{RX}} = 4.04$ Å (from a density functional B3LYP calculation), $\lambda_0 = 0.51$ eV. Thus, using the previously determined values of $\lambda^{\mathrm{el}}_{i,\mathrm{RX}} = 0.128$ eV, $\lambda^{\mathrm{el}}_{i,\mathrm{oxm}} = 1.28$ eV, we obtain $\lambda = 1.918$ eV. It follows that $k''_i = 2.3 \times 10^{-3}$ M^{-1} s^{-1}. The equilibrium constant, $k''_i/k''_{-i} = 4 \times 10^{-11}$ (from the difference between the standard potentials, $E^0_{\mathrm{RX/RX}^{\bullet -}} = -1.094$ and $E^0_{\mathrm{oxm}^{\bullet}/\mathrm{oxm}^-} = -0.49$ V vs SCE). Thus, $k''_{-i} = 5.5 \times 10^7$ M^{-1} s^{-1}.

6. Characteristic Parameters of the S_N2−ET Competition

To obtain an estimate of the *difference in potential energy between the S_N2 transition state and the ET products* we proceed in two steps: determination of the potential energy difference between the S_N2 transition state and the reactants, and, in the second step, between the ET products and the reactants.

The first of these potential energy differences may be derived as follows from the activation energy, $E_{\mathrm{A}} = 0.77$ eV (obtained as reported in section 1)[28]

$$E_{\mathrm{A}} = RT + \Delta E^{\ddagger} + \Delta H^{\ddagger}_{\mathrm{s}} + \Delta \mathrm{ZPE} - \frac{3}{2}RT - \frac{3}{2}RT + \sum_i \frac{6R\frac{h\nu_i}{k_{\mathrm{B}}}\exp\left(-\frac{h\nu_i}{k_{\mathrm{B}}T}\right)}{1 - \exp\left(-\frac{h\nu_i}{k_{\mathrm{B}}T}\right)} \quad (10)$$

(k_B, h, N_A, R: Boltzman, Planck, Avogadro, and perfect gas constants, respectively. T: absolute temperature). $\Delta E^{\ddagger}$ is the difference in electronic energy between the transition state and the reactants and $\Delta H_s^{\ddagger}$ the difference in solvation enthalpy between the same two states. ΔZPE is the difference between their zero-point energies. The two terms $(3/2)RT$ come from the translational and rotational partition functions. The last term is a vibrational contribution that may be estimated as follows.

In the reactant system, $RX + Nu^-$, there are $3 \times (N_{Nu} + N_R + N_X)$ degrees of freedom (the N's are the numbers of atoms in each moiety), which include six translations, six rotations, and $3 \times (N_{Nu} + N_R + N_X) - 12$ vibrations. Three of the later concern the cleaving bond, two bending vibrations and one stretching vibration, which is converted into an imaginary frequency vibration in the transition state. The transition state includes three translations, three rotations, and $3 \times (N_{Nu} + N_R + N_X) - 6$ vibrations. Among the later, with the exception of the six of them that come from the transformation of three of the translations and three of the rotations of the reactant system, the vibration can be approximately regarded as unchanged from the reactant to the transition state systems. Since they involve the relative movement of three large fragments, these six vibrations (five bending vibrations and the $\leftarrow Nu-R-X \rightarrow$ stretching) have low frequencies (this was confirmed by PM3 frequency calculations), thus making the vibration term in eq 10 equal to $6RT$. The ΔZPE term is very small (on the order of 10 meV from PM3 calculations). We thus find for the potential energy difference, $\Delta E^{\ddagger} = \Delta H_{s,0}^{\ddagger} = 0.67$ eV.

The potential energy difference between the ET products and the reactants was estimated as follows

$$\Delta H^0_{RX+Nu^- \rightarrow R^\bullet + Nu^\bullet + X^-} = D_{RX} - [\Delta G^0_{X^\bullet/X^-} + T(S^0_{X^\bullet} - S^0_{X^-})] + [\Delta G^0_{Nu^\bullet/Nu^-} + T(S^0_{Nu^\bullet} - S^0_{Nu^-})]$$

(H, G, and S represent the enthalpies, free enthalpies, and entropies of the subscript systems, respectively; D_{RX} is the homolytic bond dissociation energy of the R−X bond. 0 stands for standard state and s for solvation). Thus

$$\Delta H^0_{RX+Nu^- \rightarrow R^\bullet + Nu^\bullet + X^-} \approx D_{RX} - (E^0_{X^\bullet/X^-} + TS^0_{s,X^-}) + (E^0_{Nu^\bullet/Nu^-} - TS^0_{s,Nu^-})$$

Therefore, for the potential energy as the sum of an electronic energy and solvation enthalpy contributions, ΔE_{ET} and $\Delta H_{s,0}$ respectively

$$\Delta E_{ET} + \Delta H_{s,0} \approx (E_{R^\bullet} + E_{X^\bullet} - E_{RX}) - (E^0_{X/X^-} - TS^0_{s,X^-}) + (E^0_{Nu^\bullet/Nu^-} - TS^0_{s,Nu^-})$$

(E^0 is the standard potential). The solvation entropies are estimated from the equation (a is the crystallographic radii)

$$S^0_{s,anion} = S^0_{s,Cl^-} \frac{a_{Cl^-}}{a_{anion}}$$

with $S^0_{s,Cl^-} = S^0_{Cl^-,H_2O} - S^0_{Cl^-,g} + \Delta S^0_{tH_2O \rightarrow CH_3CN} = -1.55$ meV/K,[29] $a_{Cl^-} = 2.74$ Å, and $a_{Nu^-} = 3.88$ Å (derived from a volume calculation on a B3LYP/6-31G*-optimized geometry).

The standard potentials have already been estimated (Table 1), and a B3LYP/6-31G* calculation leads to $E_{R^\bullet} + E_{X^\bullet} - E_{RX} = 2.855$ eV. It follows that $\Delta E_{ET} + \Delta H_{s,0} = 0.906$ eV leading to the conclusion that the ET products are higher than the S_N2 transition state by 0.236 eV in terms of potential energy as used in the discussion in section 6.

B3LYP/6-31G* calculations have proved to give reliable estimates of the quantity $E_{R^\bullet} + E_{X^\bullet} - E_{RX} = 2.855$ in the case of benzyl chloride and substituted benzyl chlorides.[22b] Since the other parameters required for estimating the difference in potential energy between the S_N2 transition state and the ET products come from experiment, we may retain 0.24 eV as a reliable value.

In the discussion of section 6, we also needed an estimate of the bond dissociation free energy of the O-substituted product, ΔG^0_h. ΔG^0_h was estimated from B3LYP/6-31G* calculations according to the following procedure, where the solvation energies differences are neglected since all the species involved are uncharged.

$$H_{solution} \approx U_{gas}$$

Thus, the bond dissociation energy in solution, $D_{RNu \rightarrow R^\bullet + Nu^\bullet}$ may be expressed as

$$D_{RNu \rightarrow R^\bullet + Nu^\bullet} = U_{gas}(R^\bullet) + U_{gas}(Nu^\bullet) - U_{gas}(RNu)$$

$$U_{gas} = E_{elec} + E_{vib} + \frac{3}{2}RT + \frac{3}{2}RT$$

where the first term is the electronic energy and the three other the vibrational, rotational, and translational thermal energies successively. Thus, from RNu to $R^\bullet$ and $Nu^\bullet$

$$D_{RNu \rightarrow R^\bullet + Nu^\bullet} = \Delta E_{elec} + \Delta E_{vib} + 3RT$$

ΔE_{elec} and ΔE_{vib} were obtained using the B3LYP/6-31G* density functional method (geometry optimization and energy calculation).

Finally, the bond dissociation free energy was obtained from

$$\Delta G^0_h = D_{RNu \rightarrow R^\bullet + Nu^\bullet} - T[S^0_{gas}(R^\bullet) + S^0_{gas}(Nu^\bullet) - S^0_{gas}(RNu) - R\ln(22.4)]$$

the standard entropies being derived from the frequencies of the optimized geometries of each species (the term R ln(22.4) comes from the standard state being defined for a pressure of one atmosphere in the gas and for a volume of 1 L in solution).

$$\Delta G^0_{RX \rightarrow R^\bullet + X^-} = D_{RX \rightarrow R^\bullet + X^\bullet} + E^0_{RX/RX^\bullet} - - E^0_{X^\bullet/X^-} - T\Delta S_{RX \rightarrow R^\bullet + X^\bullet}$$

$$\Delta G^0_{R^\bullet + Nu^- \rightarrow RNu} = -D_{RNu \rightarrow R^\bullet + Nu^\bullet} - E^0_{RNu/RNu^{\bullet -}} + E^0_{Nu^\bullet/Nu^-} + T\Delta S_{RNu \rightarrow R^\bullet + Nu^\bullet}$$

Acknowledgment. We are indebted to Dr. M. Crozet (Université de Aix-Marseille 3) for the generous gift of a sample of 1-nitro-1,1′-dimethyl-2-(4-nitrophenyl)ethane.

JA000708D